Journal of Medicinal Chemistry Article

J. Med. Chem. **2010,** *53,* 7061–7066 **7061**
DOI: 10.1021/jm100683p

Crystal Structures of HLA-A*0201 Complexed with Melan-A/MART-$1_{26(27L)-35}$ Peptidomimetics Reveal Conformational Heterogeneity and Highlight Degeneracy of T Cell Recognition†

Céline Douat-Casassus,[‡,⊥] Oleg Borbulevych,[∥,⊥] Marion Tarbe,[‡] Nadine Gervois,[§] Francine Jotereau,[§] Brian M. Baker,*[,∥] and Stéphane Quideau*[,‡]

[‡]*Institut des Sciences Moléculaires* (*UMR-CNRS 5255*) *and Institut Européen de Chimie et Biologie* (*IECB*), *Université de Bordeaux, 2 Rue Robert Escarpit, 33607 Pessac, France,* [§]*INSERM, U601, Université de Nantes, 44322 Nantes, France, and* [∥]*Department of Chemistry and Biochemistry, University of Notre Dame, 251 Nieuwland Science Hall, Notre Dame Indiana 46556.* [⊥] *These authors have contributed equally to the work.*

Received June 7, 2010

There is growing interest in using tumor associated antigens presented by class I major histocompatibility complex (MHC-I) proteins as cancer vaccines. As native peptides are poorly stable in biological fluids, researchers have sought to engineer synthetic peptidomimetics with greater biostability. Here, we demonstrate that antigenic peptidomimetics of the Melan-A/MART-$1_{26(27L)-35}$ melanoma antigen adopt strikingly different conformations when bound to MHC-I, highlighting the degeneracy of T cell recognition and revealing the challenges associated with mimicking native peptide conformation.

Introduction

Class I major histocompatibility complex (MHC-I) proteins play a central role in immune surveillance by selectively binding antigenic peptides derived from intracellular expressed proteins.[1] After transport of the peptide−MHC-I complex (peptide−MHC-I) to the cell membrane, the cell surface is surveyed by circulating $CD8^+$ cytotoxic T lymphocytes (CTLs[a]) through their T cell receptors (TCRs). When a T cell specifically recognizes peptide−MHC-I together with costimulatory signals, a T-cell-mediated immune response is initiated, resulting in lysis of the antigen-presenting cell and initiation and propagation of an immune response. MHC-I molecules are heterodimers and comprise a membrane-linked heavy chain, a soluble light chain (β_2-microglobulin), and a short peptide, typically 8−10 amino acids in length. The peptide binding site is constructed as a groove formed by the α1 and α2 helices supported by a β sheet of the heavy chain. Peptide specificity for MHC-I is conferred by two dominant anchor residues (P2 and PΩ for the C-terminal position),[2] while TCR antigen specificity is largely determined by the solvent-exposed side chains of the peptide central core.[3] Generally, antigenic peptides bind to MHC-I proteins in an extended conformation with the peptide central core bulging out or even zigzagging within the binding groove.

Since their first identification in the early 1990s, tumor-associated antigenic (TAA) peptides have been considered as promising candidates for the development of cancer vaccines. However, their weak immunogenicity and their high sensitivity to proteases have limited the success of synthetic TAA peptides as immunotherapeutic agents. Effort has therefore been devoted to modifying naturally occurring TAA peptides to design more biologically stable analogues for immunotherapeutic applications.

The Melan-A/MART-1 protein antigen (hereafter referred to as Melan-A) is up-regulated in about 89% melanoma cell lines[4] and elicits natural $CD8^+$ T cell responses.[5] Screening of peptides derived from Melan-A led to the identification of the immunodominant peptide epitope comprising residues 26−35 (EAAGIGILTV), for which T cell recognition is restricted by the human leukocyte antigen (HLA)-A*0201 (HLA-A2). A drawback of this epitope is its moderate HLA-A2 binding affinity due to the absence of an optimal residue at the second anchor residue (P2). Replacement of the P2 alanine by leucine to yield the altered Melan-$A_{26(27L)-35}$ peptide (ELAGIGILTV, referred to as ELA-**0**)[6] resulted in enhanced HLA-A2-binding affinity and improved immunogenicity with T cells specific for the native EAA decamer. Consequently, the ELA-**0** peptide has been and continues to be used in numerous clinical trials for the immunological treatment of melanoma.[7] Unfortunately, as with most peptides used in immunological treatments, the ELA-**0** peptide exhibits poor stability in biological fluids.[8] In this context, the design of new synthetic, bioresistant ELA-**0** analogues presents an opportunity for the development of more effective immunologically based therapies targeting melanoma.

Over the past few years, attempts have been made to replace protease-susceptible peptide bonds in the ELA-**0** peptide with their corresponding isosteres or non-natural amino acids.[8,9] We recently investigated a strategy involving substitution of the TCR-contacting central amino acids with protease

†The crystal structures of HLA-A*0201 complexed with Melan-A/MART-$1_{26(27L)-35}$ peptidomimetics have been deposited (PDB codes 3O3A, 3O3B, 3O3D, and 3O3E, respectively).

*To whom correspondence should be addressed. For B.M.B.: phone, (574) 631 9810; fax, (574) 631 6652; e-mail, brian-baker@nd.edu. For S.Q.: phone, +33 (0) 540 00 30 10; fax, +33 (0) 540 00 22 15; e-mail, s.quideau@iecb.u-bordeaux.fr.

[a]Abbreviations: AMBA, 3-aminomethylbenzoic acid; CTL, cytotoxic T lymphocyte; DMSO, dimethyl sulfoxide; HLA, human leukocyte antigen; MES, 2-(*N*-morpholino)ethanesulfonic acid; MHC, major histocompatibility complex; PEG, polyethylene glycol; rmsd, root-mean-square deviation; RP-HPLC, reverse phase high performance liquid chromatography; TAA, tumor associated antigen; TLS, translation, libration, and screw; TCR, T cell receptor.

Published on Web 08/31/2010

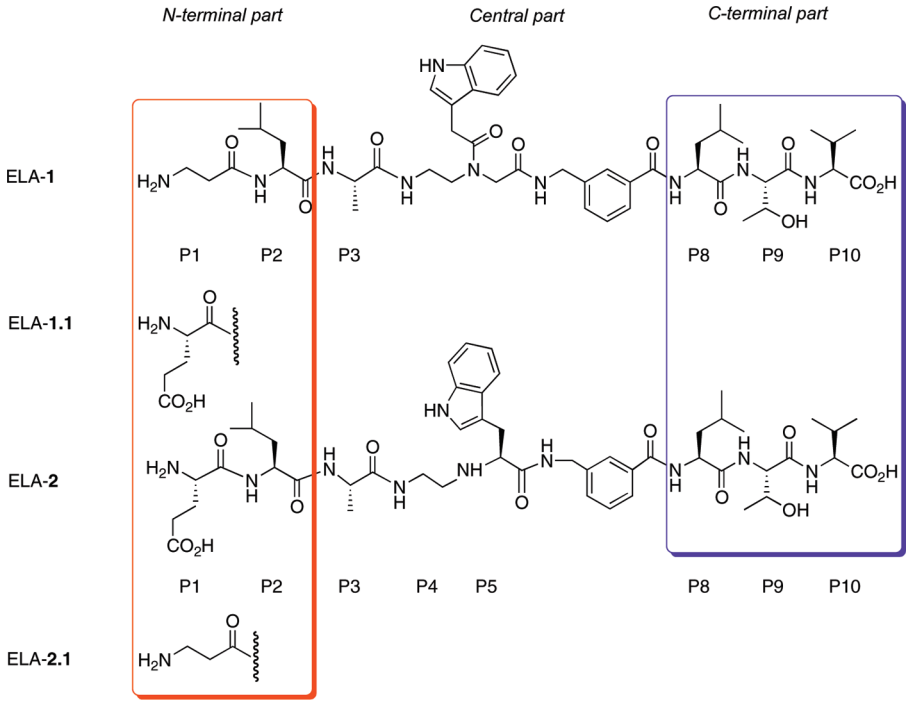

Figure 1. Chemical structures of the four ELA analogues showing the chemical differences in the central TCR-contacting and N-terminal parts.

resistant, nonpeptidic motifs potentially capable of making improved interactions with the TCR.[10] Through an in silico design approach, the central GIGI tetrapeptide of ELA-**0** was replaced with pseudopeptidic units equipped with different organic haptens. To further enhance biostability, some of our analogues also had a β-alanine at P1 in place of the native glutamate (Figure 1).[8]

Notably, despite the drastic modifications made to the ELA-**0** central core, the majority of our synthetic analogues had similar or even improved binding affinity with the HLA-A2 molecule. Moreover, some of our peptidomimetics retained reactivity with Melan-A-specific T cell clones.[10]

Here, we sought to identify how chemical modifications of ELA-**0** alter its presentation by the HLA-A2 molecule with the aim of gaining further insight into the potential use of peptidomimetics as immunotherapeutic agents. Toward this end, we determined the crystallographic structures of our two most successful ELA-**0** based peptidomimetics bound to HLA-A2 (ELA-**1** and ELA-**2** in Figure 1). We also explored the structural consequences of the modifications made to the N-terminal part as a means to enhance exoprotease resistance.[8]

The structures revealed (1) variations in the presentation of the peptidomimetics, both with respect to each other and with respect to the native ELA-**0** peptide, highlighting the challenges associated with mimicking the conformations of native peptides in MHC-I binding grooves, (2) the capacity for antigen-specific T cell receptors to cross-react with structurally diverse ligands. The structures also revealed that the modification of peptide N-termini made to enhance protease resistance can have unintended structural consequences. Beyond unveiling the complexity of these structural modulations, our results provide a concrete starting point for structure-based enhancement of synthetic mimics of natural antigenic peptides.

Results

The four ELA-**0**-based peptidomimetics examined are shown in Figure 1 and termed ELA-**1**, ELA-**1.1**, ELA-**2**, and ELA-**2.1**. ELA-**1** was referred to as compound **21** in our previous work, whereas ELA-**2** was referred to as compound **6**.[10] Both ELA-**1** and ELA-**2** strongly activated two ELA-**0** specific T cell clones. ELA-**1.1** and ELA-**2.1** are derivatives of ELA-**1** and ELA-**2** that either retain the native glutamate at the N-terminus (ELA-**1.1**) or include a β-alanine (ELA-**2.1**) at this position.

All four peptidomimetic/HLA-A2 complexes crystallized in the same $P2_1$ space group with two molecules per asymmetric unit, as seen with other HLA-A2 complexes, including the complex with the native ELA-**0** peptide.[11,12] The four new complexes maintained the typical peptide/HLA-A2 architecture, with no perturbation to the secondary structure that forms the HLA-A2 peptide binding groove. However, important structural differences were seen in the various structures as described below. Diffraction data and refinement statistics for all four structures are shown in Table 1.

Structures of ELA-1 and ELA-1.1 Bound to HLA-A2. In ELA-**1**, the central GIGI tetrapeptide is replaced with a 3-aminomethylbenzoic acid (AMBA) spacer combined with *N*-(2-aminoethyl)glycine unit bearing a tryptophan-like side chain that extends away from the backbone by an additional carbonyl unit. The N-terminal glutamate is also replaced with a protease-resistant β-alanine. The structure of ELA-**1** bound to HLA-A2 was solved to 1.8 Å (Table 1). The two molecules in the unit cell were essentially identical, with all atoms of the two copies of the constructs superimposing with an rmsd of 0.3 Å.

In the initial in silico design of ELA-**1**, the AMBA spacer was predicted to be buried in the base of the peptide binding groove and the indole acetyl side chain was predicted to point away from the groove, facilitating interactions with incoming

Table 1. X-ray Data and Refinement Statistics

protein	ELA-**1**/HLA-A2	ELA-**1.1**/HLA-A2	ELA-**2**/HLA-A2	ELA-**2.1**/HLA-A2
PDB entry	3O3A	3O3B	3O3D	3O3E
radiation source (beamline)	APS (19BM)	APS (14BM)	APS (19BM)	APS (14BM)
space group	$P2_1$	$P2_1$	$P2_1$	$P2_1$
a (Å)	58.2	58.1	58.2	58.2
b (Å)	84.2	84.3	84.2	84.4
c (Å)	84.0	84.0	84.1	84.0
β (deg)	90.0	90.0	90.1	90.1
molecules/asymmetric unit	2	2	2	2
resolution (Å)	20−1.8	20−1.9	20−1.7	20−1.9
total no. of reflections	74605	61720	88669	66944
mosaicity (deg)	0.28	0.38	0.30	0.23
completeness[a] (%)	99.5 (96.2)	96.9 (81.6)	99.4 (98.3)	96.5 (72.9)
I/σ	13.4 (1.7)	10.9 (2.1)	17.7 (2.0)	14.5 (1.7)
R_{merge} (%)	9.2 (51.1)	14.1 (49.7)	9.1 (49.6)	10.8 (63.4)
average redundancy	3.6 (3.3)	3.6 (3.1)	3.6 (3.2)	3.6 (2.7)
R_{work} (%) (no. reflections)	17.1 (71352)	18.6 (58568)	18.0 (84177)	18.2 (63539)
R_{free} (%) (no. reflections)	21.2 (3786)	23.8 (3116)	21.8 (4435)	22.9 (3377)
$\langle B \rangle$ (all atoms) (Å^2)	21.1	11.6	16.9	17.4
Ramachandran plot				
most favored (%)	92.2	91.6	93.1	91.8
allowed (%)	7.5	8.1	6.6	7.9
generously allowed (%)	0.3	0.3	0.3	0.3
RMS deviations from ideality				
bond (Å)	0.016	0.018	0.016	0.017
angle (deg)	1.762	1.843	1.704	1.719
coordinate error[b] (Å)	0.09	0.12	0.08	0.11

[a] Numbers in parentheses refer to the highest resolution shell. [b] Mean estimate based on maximum likelihood methods.

T cell receptors.[10] However, the ELA-**1**/HLA-A2 structure revealed almost the opposite: the AMBA spacer instead bulges up and out of the groove, and the indole unit, rather than pointing away from the peptide binding groove, points toward the HLA-A2 α1 helix and lies partially underneath the AMBA spacer (Figure 2a).

As a decameric peptide, the center of the ELA-**0** peptide zigzags throughout the HLA-A2 peptide binding groove. The center of ELA-**1** also zigzags but does so in the opposite direction, bending toward and above the α1 helix at the AMBA spacer (Figure 2a). Overall, the path adopted by ELA-**1** through the HLA-A2 peptide binding groove diverges substantially from that of ELA-**0**, especially in the region replaced by the synthetic spacer. For example, the distance between the nitrogen of the AMBA spacer of ELA-**1** and that of Gly6 of ELA-**0**, intended to occupy similar positions, is 6.7 Å.

The replacement of the native glutamate with a β-alanine at the N-terminus had significant structural consequences. Compared to a standard amino acid, β-alanine introduces an additional carbon−carbon bond between the first carbonyl oxygen and the peptidomimetic N-terminus (Figure 1). As shown in Figure 2b, in the ELA-**1**/HLA-A2 structure, this additional bond forces the N-terminus out of the HLA-A2 P1 pocket, resulting in the loss of a hydrogen bond to Tyr171 of the HLA-A2 heavy chain that is conserved in all peptide/HLA-A2 structures in which the P1 pocket is occupied. The N-terminus instead points up out of the pocket, displacing the side chain of Lys66 by 3.2 Å because of charge and steric repulsions. This remarkable movement of Lys66 results in the loss of another conserved peptide-HLA-A2 hydrogen bond, from Lys66 to the carbonyl oxygen of the leucine at peptide position 2. The shift in Lys66 also removes a salt bridge made with Glu63 that is conserved in the majority of peptide/HLA-A2 complexes.[13,14]

Although ELA-**1** bound well to HLA-A2 and was recognized by Melan-A specific T cell clones, the alterations in conserved hydrogen bonds and salt bridges around the peptidomimetic N-terminus could significantly impact peptide and TCR binding for other systems.[13,15] We thus asked whether the alterations could be reversed by reverting to a native glutamate at the first position. The resulting ELA-**1.1** peptide is identical to ELA-**1** except that the β-alanine at P1 is replaced with glutamate (Figure 1).

The structure of ELA-**1.1**, determined at 1.9 Å (Table 1), was identical to that of ELA-**1** except for the region around the N-terminus, which indeed showed a return to a "normal" N-terminal environment, with the hydrogen bond between the N-terminus and Tyr171, the hydrogen bond between the Leu2 oxygen and Lys66, and the salt bridge between Lys66 and Glu63 all formed (Figure 2c). Thus, the N-terminal structural alterations in the ELA-**1** structure are all attributable to the presence of the β-alanine.

Structures of ELA-2 and ELA-2.2 Bound to HLA-A2. The ELA-**2** peptidomimetic also included the AMBA spacer but combined it with a reduced peptide bond introduced between the glycine at P4 and a standard tryptophan at P5 (Figure 1). Unlike ELA-**1**, ELA-**2** retained the native glutamate at the N-terminus as it was designed earlier.[10] As with ELA-**1**, ELA-**2** adopted a different path through the HLA-A2 peptide binding groove compared to the ELA-**0** peptide. Rather than zigzagging, the center of ELA-**2** simply bulged out such that the conformation of the ELA-**2** central part was somewhat between that of ELA-**0** and ELA-**1** (Figure 3a). The two molecules in the ELA-**2** asymmetric unit positioned the AMBA spacer and the preceding peptide bond unit in different conformations, and in one of the molecules in the asymmetric unit, the side chains and backbones of Leu8 and Thr9 could be refined in two conformations (Figure 3b). Together, this represents a degree of conformational heterogeneity present with ELA-**2** but not with ELA-**1**. One of the AMBA positions in ELA-**2** closely (within 2 Å) mimicked the position of the AMBA spacer in ELA-**1** (shown in Figure 3a).

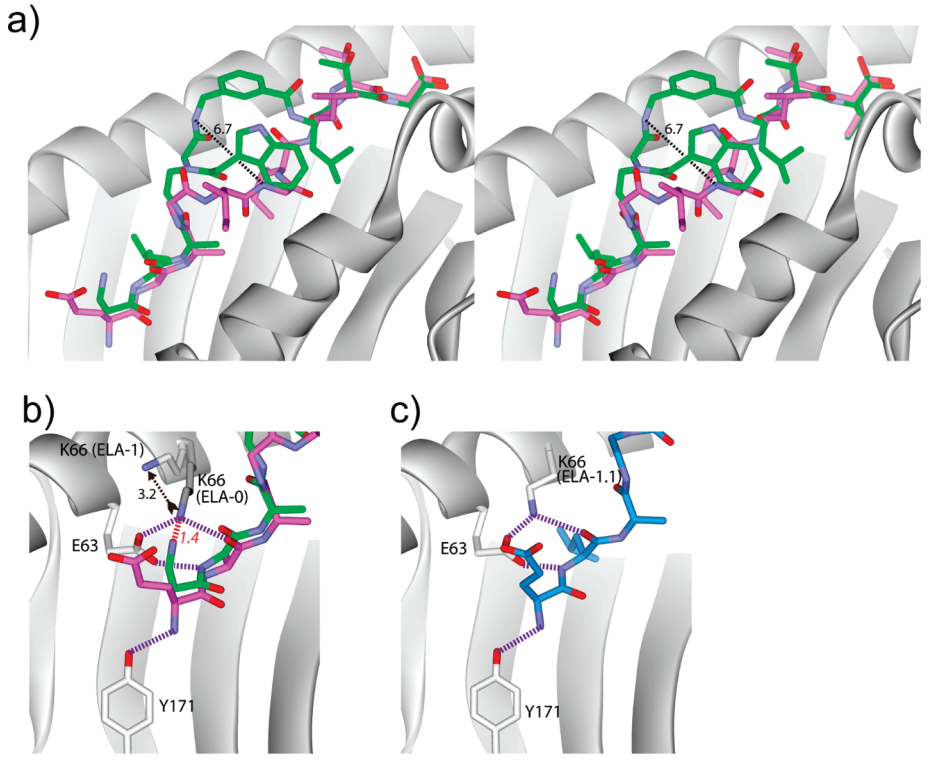

Figure 2. Structural comparison of the ELA-**1** and ELA-**1.1** mimetics with the native ELA-**0** peptide. (a) Cross-eyed stereo comparison of ELA-**1** with ELA-**0** in the HLA-A2 peptide binding groove. ELA-**1** diverges substantially from ELA-0, particularly in the central portion of the molecule. ELA-**0** is purple and ELA-**1** is green. (b) The nitrogen of the β-alanine in ELA-**1** points out of the P1 pocket, forcing a repositioning of Lys66 and disrupting the traditional N-terminal hydrogen bonding arrangement. Hydrogen bonds are purple, and the clash between β-alanine and Lys66 is illustrated in red. A hydrogen bond between Lys66 and Glu1 in the ELA-**1.1** structure is not shown for clarity. (c) The ELA-**1.1** compound, which replaces the β-alanine of ELA-**1** with glutamate, restores the normal position of Lys66 and the traditional hydrogen bonding arrangement. Superimpositions for all panels are through the backbones of the peptide binding domains.

Interestingly, the side chain of Trp5 angled into the same position as the indole ring in ELA-**1**, reflecting a preference for an aromatic side chain at the position 5 pocket in HLA-A2.[16]

Unlike ELA-**1**, ELA-**2** retained the native glutamate at the N-terminus. As anticipated from the results with ELA-**1** and ELA-**1.1**, the normal position of Lys66 and the hydrogen bonding/salt-bridge network around the N-terminus were retained in the ELA-**2** structure. To verify conclusively that the rearrangements seen in ELA-**1** were due to the use of β-alanine and not influenced by other modifications, we examined a version of ELA-**2** that replaced the native glutamate with a β-alanine (ELA-**2.1** in Figure 1). The structure of ELA-**2.1** bound to HLA-A2 revealed structural consequences identical to those seen with ELA-**1**: loss of the N-terminal hydrogen bond to Tyr171 and a rearrangement of Lys66, resulting in the loss of the hydrogen bond to position 2 and the salt bridge with Glu63 (Figure 3c).

Discussion

With the growing use of tumor associated antigens as the basis for the development of vaccines for cancer and infectious diseases,[17] there has been a concomitant interest in the development of synthetic analogues or peptidomimetics with greater biological stability or immunological potency. Our mimetics of the Melan-$A_{26(27L)-35}$ tumor antigen (ELA-**0**) bound well to HLA-A2 and activated Melan-A-specific T cells,[10] demonstrating an important proof of principle and providing a platform on which further development can be based.

Surprisingly, the structures of our two most promising peptidomimetics (ELA-**1** and ELA-**2**) bound to HLA-A2 determined here revealed crucial differences in the central AMBA-substituted portion of the peptide when compared to the structure with the ELA-**0** peptide, after which they were modeled. These differences highlight the capacity of our AMBA-based mimetics to alter their conformation to correctly position their primary anchors to achieve tight binding to HLA-A2.

But given the different structures for ELA-**1** and ELA-**2**, how is it that they are able to stimulate ELA-**0**-specific T cells? One important clue may lie in the conformational diversity observed in the ELA-**2**/HLA-A2 crystal structure. Several studies have shown that the adaptability of antigenic peptides can lead to the formation of stable TCR−pMHC interfaces, most recently with ligands with little structural homology in the TCR-free state.[18] Alternatively, the TCRs responsible for cross-recognition between ELA-**0** and ELA-**1**/ELA-**2** may possess flexible CDR loops that permit recognition of disparate structures.[19] Indeed, cross-reactivity with structurally disparate ligands is a hallmark of Melan-A_{26-35}-specific TCRs, as they readily cross-react with the 27−35 epitope, which as a nonamer adopts a different path through the HLA-A2 peptide binding groove as does the 26−35 decamer.[20] It is possible that cross-reactivity between ELA-**0** and ELA-**1**/ELA-**2** proceeds via a combination of peptide and TCR conformational adaptability, as recently demonstrated with variants and mimics of the HTLV-1 Tax_{11-19} peptide.[21,22] A more complete understanding of the mechanism by which ELA-**1** and ELA-**2** are recognized will require solution

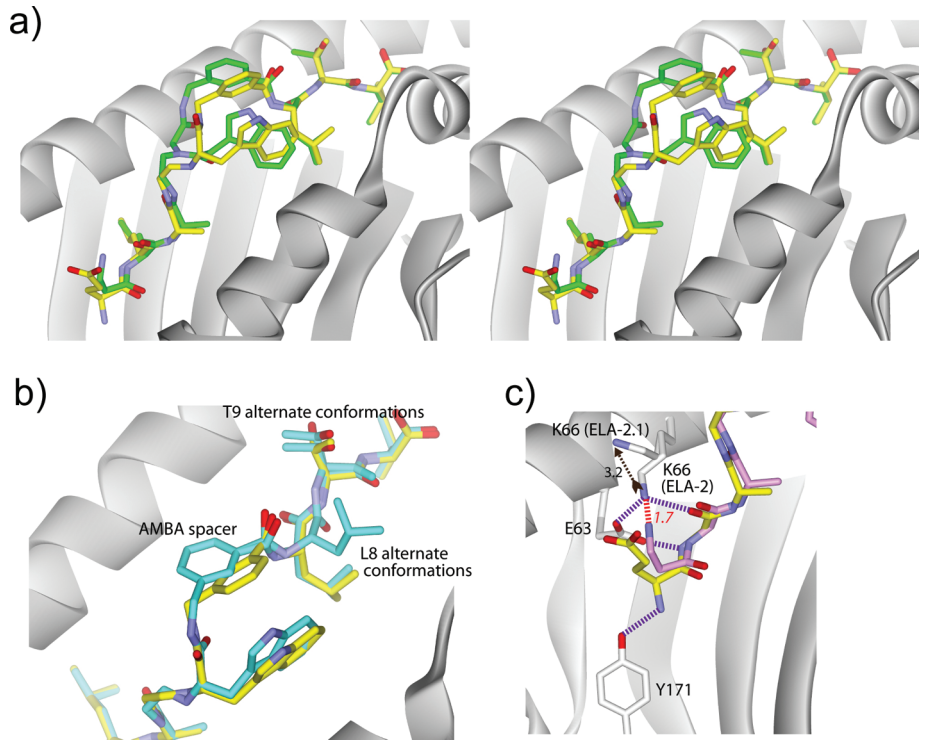

Figure 3. Structural comparison of the ELA-**1** and ELA-**2** peptidomimetics. (a) Cross-eyed stereocomparison of ELA-**1** and ELA-**2** in the HLA-A2 peptide binding groove. Unlike ELA-**1**, ELA-**2** does not zigzag but instead bulges straight from the center of the groove. ELA-**2** is yellow and ELA-**1** is green. (b) ELA-**2** shows conformational heterogeneity in the HLA-A2 binding groove. The AMBA spacer occupies two different conformations in the two molecules in the asymmetric unit (yellow and cyan). The first molecule in the asymmetric unit (cyan) displayed alternative conformations for the backbones and side chains of Leu8 and Thr9. (c) The structure with the ELA-**2.1** mimetic, which replaced the N-terminal glutamate of ELA-**2** with β-alanine, revealed an altered position for Lys66 and disrupted N-terminal hydrogen bonding arrangement, similar to that seen in the structure with ELA-**1**. ELA-**2** is yellow, and ELA-**2.1** is pink. Hydrogen bonds are purple, and the clash between β-alanine and Lys66 is illustrated in red. A hydrogen bond between Lys66 and Glu1 in the ELA-**2** structure is not shown for clarity. Superimpositions for all panels are through the backbones of the peptide binding domains.

of crystal structures of the TCR−peptide−MHC ternary complexes.

A second key result revealed by the crystallographic structures is the structural consequences of using a β-alanine at the N-terminus. β-Alanine was used to enhance resistance to exoproteases. However, the structures showed unambiguously that β-alanine disrupted the conformation at the N-terminus, resulting in the loss of hydrogen bonds and altering the position of Lys66. Although this did not appear to negatively affect the binding of our compounds to HLA-A2, nor did it disrupt recognition by two different T cell clones, this should not be expected in all cases. Lys66 is a key amino acid in several interfaces that TCRs form with HLA-A2, and alterations to Lys66 have been linked to a loss in recognition in other cases.[14] Thus, caution should be used when considering β-alanine or similar non-native amino acids at the N-terminus of peptidomimetics.

Conclusions

In summary, we have determined the crystallographic structures of two promising peptidomimetics of the Melan-A_{26-35} tumor antigen to HLA-A2. Although the conformations in the peptide binding groove diverged from that of the native peptide, HLA-A2 binding and, for at least two T cell clones, TCR recognition were maintained.[10] This structural analysis underscores the degeneracy present in TCR recognition of ligand. Furthermore, such degeneracy being difficult to predict, this work highlights the difficulties in designing close structural mimics of antigenic peptides. Nonetheless, our results provide a concrete starting point for the structure-based enhancement of synthetic mimics of Melan-A/MART-1 epitopes capable of being recognized by human TCRs in a HLA-A2-restricted context.[23]

Experimental Methods

Synthesis. We have reported the synthesis of ELA-**1** and ELA-**2** in a previous publication.[10] The compounds were determined to be >95% pure by RP-HPLC. Detailed procedure for the solid phase synthesis of their derivatives ELA-**1.1** and ELA-**2.2** is described in the Supporting Information. Both peptidomimetics were obtained with purities of >95%.

Protein Expression, Purification, and Crystallization. The extracellular domains of HLA-A2 and β_2-microglobulin were expressed in *Escherichia coli* as inclusion bodies, refolded with excess peptidomimetic dissolved in DMSO, and chromatographically purified as described previously.[24] The HLA-A2 complexes were crystallized at 4 °C from a precipitant solution of 24% PEG3350, 0.1 M KCl or NaF, buffered with 0.025 M MES at pH 6.5 using sitting drop/vapor diffusion. Seeding was used to obtain higher quality single crystals.

Data Collection, Structure Solution, and Refinement. For data collection, crystals were transferred to mother liquor supplemented with 20% of glycerol and flash-frozen in liquid nitrogen. Diffraction data were collected at the indicated beamlines (Table 1). Data collection statistics are given in Table 1. Oscillation frames were integrated and scaled with HKL2000.[25] Structures were solved by molecular replacement with MOLREP[26] using PDB code 2GT9[19] as a search model with the coordinates for the peptide excluded. Rigid body refinement, TLS refinement,

and restrained refinement were performed with Refmac5[27] as incorporated in CCP4-6.0.2. The TLS groups for refinement were chosen as previously described.[21] Once refined, TLS parameters were included in all subsequent refinement steps. Anisotropic and bulk solvent corrections were performed throughout refinement. Water was added using ARP/wARP.[28] Graphical evaluation of the model and fitting to maps were performed using Coot[29] and XtalView.[30] The quality of the structures during refinement was monitored with the Coot validation engine and Procheck.[31] Structure factors and coordinates have been submitted to the Protein Data Bank; PDB codes are listed in Table 1.

Acknowledgment. The authors thank the Servier Laboratories and the Société Française de Chimie Thérapeutique for financial support and M.T.'s research assistantship. O.Y.B. was supported by the Walther Cancer Foundation. This work was supported by Grant GM067079 from NIGMS, NIH (U.S.) and Grant RSG-05-202-01-GMC from the American Cancer Society. Results shown in this report are derived from work performed at Argonne National Laboratory, Structural Biology Center at the Advanced Photon Source. Argonne is operated by UChicago Argonne, LLC, for the U.S. Department of Energy, Office of Biological and Environmental Research under Contract DE-AC02-06CH11357. Use of the BioCARS Sector 14 was supported by the NCRR, NIH, U.S., under Grant RR007707.

Supporting Information Available: Detailed procedure of the solid phase synthesis of the four peptidomimetics and X-ray electron density images. This material is available free of charge via the Internet at http://pubs.acs.org.

References

(1) Peaper, D. R.; Cresswell, P. Regulation of MHC class I assembly and peptide binding. *Annu. Rev. Cell Dev. Biol.* **2008**, *24*, 343–368.
(2) Rammensee, H. G.; Falk, K.; Rotzschke, O. Peptides naturally presented by MHC class I molecules. *Annu. Rev. Immunol.* **1993**, *11*, 213–244.
(3) (a) Garcia, K. C.; Teyton, L.; Wilson, I. A. Structural basis of T cell recognition. *Annu. Rev. Immunol.* **1999**, *17*, 369–397. (b) Rudolph, M. G.; Wilson, I. A. The specificity of TCR/pMHC interaction. *Curr. Opin. Immunol.* **2002**, *14*, 52–65.
(4) Murer, K.; Urosevic, M.; Willers, J.; Selvam, P.; Laine, E.; Burg, G.; Dummer, R. Expression of Melan-A/MART-1 in primary melanoma cell cultures has prognostic implication in metastatic melanoma patients. *Melanoma Res.* **2004**, *14*, 257–262.
(5) Pittet, M. J.; Valmori, D.; Dunbar, P. R.; Speiser, D. E.; Liénard, D.; Lejeune, F.; Fleischhauer, K.; Cerundolo, V.; Cerottini, J. C.; Romero, P. High frequencies of naive Melan-A/MART-1-specific CD8+ T cells in a large proportion of human histocompatibility leukocyte antigen (HLA)-A2 individuals. *J. Exp. Med.* **1999**, *190*, 705–715.
(6) Valmori, D.; Fonteneau, J. F.; Maranon Lizana, C.; Gervois, N.; Liénard, D.; Rimoldi, D.; Jongeneel, C. V.; Jotereau, F.; Cerottini, J. C.; Romero, P. Enhanced generation of specific tumor-reactive CTL in vitro by selected Melan-A/MART-1 immunodominant peptide analogs. *J. Immunol.* **1998**, *160*, 1750–1758.
(7) Nisticò, P.; Capone, I.; Palermo, B.; Del Bello, D.; Ferraresi, V.; Moschella, F.; Aricò, E.; Valentini, M.; Bracci, L.; Cognetti, F.; Ciccarese, M.; Vercillo, G.; Roselli, M.; Fossile, E.; Tosti, M. E.; Wang, E.; Marincola, F.; Imberti, L.; Catricalà, C.; Natali, P. G.; Belardelli, F.; Proietti, E. Chemotherapy enhanced vaccine-induced immunity in melanoma patients. *Int. J. Cancer* **2009**, *124*, 130–139.
(8) Blanchet, J. S.; Valmori, D.; Dufau, I.; Ayyoub, M.; Nguyen, C.; Guillaume, P.; Monsarrat, B.; Cerottini, J. C.; Romero, P.; Gairin, J. E. A new generation of Melan-A/MART-1 peptides that fulfill both increased immunogenicity and high resistance to biodegradation: implication for molecular anti-melanoma immunotherapy. *J. Immunol.* **2001**, *167*, 5852–5861.
(9) Quesnel, A.; Zerbib, A.; Connan, F.; Guillet, J. G.; Briand, J. P.; Choppin, J. Synthesis and antigenic properties of reduced peptide bond analogues of an immunodominant epitope of the melanoma MART-1 protein. *J. Pept. Sci.* **2001**, *7*, 157–165.
(10) Douat-Casassus, C.; Marchand-Geneste, N.; Diez, E.; Gervois, N.; Jotereau, F.; Quideau, S. Synthetic anticancer vaccine candidates: rational design of antigenic peptide mimetics that activate tumor-specific T-cells. *J. Med. Chem.* **2007**, *50*, 1598–1609.
(11) Sliz, P.; Michielin, O.; Cerottini, J. C.; Luescher, I.; Romero, P.; Karplus, M.; Wiley, D. C. Structures of two closely related but antigenically distinct HLA-A2/melanocyte-melanoma tumor-antigen peptide complexes. *J. Immunol.* **2001**, *167*, 3276–3284.
(12) Borbulevych, O. Y.; Insaidoo, F. K.; Baxter, T. K.; Powell, D. J., Jr.; Johnson, L. A.; Restifo, N. P.; Baker, B. M. Structures of MART-$1_{26/27\text{-}35}$ peptide/HLA-A2 complexes reveal a remarkable disconnect between antigen structural homology and T cell recognition. *J. Mol. Biol.* **2007**, *372*, 1123–1136.
(13) Baxter, T. K.; Gagnon, S. J.; Davis-Harrison, R. L.; Beck, J. C.; Binz, A. K.; Turner, R. V.; Biddison, W. E.; Baker, B. M. Strategic mutations in the class I major histocompatibility complex HLA-A2 independently affect both peptide binding and T cell receptor recognition. *J. Biol. Chem.* **2004**, *279*, 29175–29184 and references cited therein.
(14) Gagnon, S. J.; Borbulevych, O. Y.; Davis-Harrison, R. L.; Baxter, T. K.; Clemens, J. R.; Armstrong, K. M.; Turner, R. V.; Damirjian, M.; Biddison, W. E.; Baker, B. M. Unrevealing a hotspot for TCR recognition on HLA-A2: evidence against the existence of peptide-independent TCR binding determinants. *J. Mol. Biol.* **2005**, *353*, 556–573 and references cited therein.
(15) Bouvier, M.; Wiley, D. C. Importance of peptide amino and carboxyl termini to the stability of MHC class I molecules. *Science* **1994**, *265*, 398–402.
(16) Madden, D. R. The three-dimensional structure of peptide−MHC complexes. *Annu. Rev. Immunol.* **1995**, *13*, 587–622.
(17) Purcell, A. W.; McCluskey, J.; Rossjohn, J. More than one reason to rethink the use of peptides in vaccine design. *Nat. Drug Discovery* **2007**, *6*, 404–414.
(18) Macdonald, W. A.; Chen, Z.; Gras, S.; Archbold, J. K.; Tynan, F. E.; Clements, C. S.; Bharadwaj, M.; Kjer-Nielsen, L.; Saunders, P. M.; Wilce, M. C. J.; Crawford, F.; Stadinsky, B.; Jackson, D.; Brooks, A. G.; Purcell, A. W.; Kappler, J. W.; Burrows, S. R.; Rossjohn, J.; McCluskey, J. T cell allorecognition via molecular mimicry. *Immunity* **2009**, *31*, 897–908.
(19) Armstrong, K. M.; Piepenbrink, K. H.; Baker, B. M. Conformational changes and flexibility in T-cell receptor recognition of peptide−MHC complexes. *Biochem. J.* **2008**, *415*, 183–196.
(20) Borbulevych, O. Y.; Insaidoo, F. K.; Baxter, T. K.; Powell, D. J., Jr.; Johnson, L. A.; Restifo, N. P.; Baker, B. M. Structures of MART-1(26/27-35) peptide/HLA-A2 complexes reveal a remarkable disconnect between antigen structural homology and T cell recognition. *J. Mol. Biol.* **2007**, *372*, 1123–1136.
(21) Gagnon, S. J.; Borbulevych, O. Y.; Davis-Harrison, R. L.; Turner, R. V.; Damirjian, M.; Wojnarowicz, A.; Biddison, W. E.; Baker, B. M. T cell receptor recognition via cooperative conformational plasticity. *J. Mol. Biol.* **2006**, *363*, 228–243.
(22) Borbulevych, O. Y.; Piepenbrink, K. H.; Gloor, B. E.; Scott, D. R.; Sommese, R. F.; Cole, D. K.; Sewell, A. K.; Baker, B. M. T cell receptor cross-reactivity directed by antigen-dependent tuning of peptide−MHC molecular flexibility. *Immunity* **2009**, *31*, 885–896.
(23) Cole, D. K.; Yuan, F.; Rizkallah, P. J.; Miles, J. J.; Gostick, E.; Price, D. A.; Gao, G. F.; Jakobsen, B. K.; Sewell, A. K. Germ line-governed recognition of a cancer epitope by an immunodominant human T-cell receptor. *J. Biol. Chem.* **2009**, *284*, 27281–27289.
(24) Davis-Harrison, R. L.; Armstrong, K. M.; Baker, B. M. Two different T cell receptors use different thermodynamic strategies to recognize the same peptide/MHC ligand. *J. Mol. Biol.* **2005**, *346*, 533–550.
(25) Otwinowski, Z.; Minor, W. Processing of X-ray diffraction data collected in oscillation mode. *Methods Enzymol.* **1997**, *276*, 307–326.
(26) Vagin, A.; Teplyakov, A. Molecular replacement with MOLREP. *Acta Crystallogr., Sect. D: Biol. Crystallogr.* **2010**, *66*, 22–25.
(27) Murshudov, G. N.; Vagin, A. A.; Dodson, E. J. Refinement of macromolecular structures by the maximum-likelihood method. *Acta Crystallogr., Sect. D: Biol. Crystallogr.* **1997**, *53*, 240–255.
(28) Perrakis, A.; Sixma, T. K.; Wilson, K. S.; Lamzin, V. S. wARP: improvement and extension of crystallographic phases by weighted averaging of multiple-refined dummy atomic models. *Acta Crystallogr., Sect. D: Biol. Crystallogr.* **1997**, *53*, 448–455.
(29) Emsley, P.; Cowtan, K. Coot: model-building tools for molecular graphics. *Acta Crystallogr., Sect. D: Biol. Crystallogr.* **2004**, *60*, 2126–2132.
(30) McRee, D. E. XtalView/Xfit−a versatile program for manipulating atomic coordinates and electron density. *J. Struct. Biol.* **1999**, *125*, 156–165.
(31) Laskowski, R. A.; MacArthur, M. W.; Moss, D. S.; Thornton, J. M. PROCHECK: a program to check the stereochemical quality of protein structures. *J. Appl. Crystallogr.* **1993**, *26*, 283–291.